CHAPTER V

EFFECT OF SILVER NANOPARTICLES ON POLYMER BLENDED REDUCED GRAPHENE NANOHYBRIDS AS A VERSATILE ELECTROCHEMICAL SENSOR FOR THE DETECTION OF p-AMINOPHENOL

5.1 INTRODUCTION

In recent years, polymer nanocomposites have become a vital focus in the polymeric field. Owing to their outstanding properties and potential applications most of the researches are focused on polymer-matrix nanocomposites [1]. Graphene, a 2D sp^2 hybridized carbon atoms densely arranged in an honeycomb lattice has attracted enomorous attention in scientific and research areas due to its extraordinary properties like high electron mobility, mechanical stiffness, electronic transport and high electrical conductivity [2]. Graphene oxide (GO) is one of the most important derivatives of graphene, consisting of a layered structure with a hexagonal ring of carbon network and oxygen functional groups bearing on the basal planes and edges, that are well dispersed in multiple polar mediums [3-4] . These properties make them ideal candidates for modifying agents for polymers. The integration of nanomaterials in a polymer matrix has opened up a new and interesting area in research field [5]. Chitosan is a 2-amino-2-deoxy-(1, 4)-β-D-linked polyaminosaccharide natural biopolymer, normally obtained by the alkaline deacetylation of chitin. The activities of its free amino groups are much higher than its hydroxyl groups which are feasible for chemical modifications under normal conditions. The chitosan-functionalized reduced graphene oxide electrode facilitates the electron transfer rate at the electrode surface through the π-π stacking interaction and electrostatic attraction, thus enhances the electrochemical performance for sensing applications. [6].The deposition of inorganic materials such as metallic, semiconducting and insulating nanoparticles onto the graphene nanosheets increases the surface area and active sites for binding analyte. The conductivity as well as the mechanical strength of the biosensor exhibits a greater sensitivity for the detection of a variety of biomolecules [7]. Over the past few decades, silver nanoparticles have been focused intensively due to their unique properties such as electrical,

optical, sensing, catalytic, antibacterial properties that differ from that of bulk materials [8].

An aromatic phenolic compound, p-aminophenol (p-AP) has been primarily used in various industrial fields such as petroleum, dye, polymers and also for the production of paracetomol [9]. However, it is a hydrolytic product of acetaminophen that has serious nephrotoxic and teratogenic effects and has been observed as a synthetic intermediate, which is dangerous to human body that causes irritation to eyes, skin, and respiratory system [10]. Due to its nephrotoxicity, it has a great ability to cause methemoglobinemia in animals. It is treated as an environmental pollutant as it has high release in petroleum additives, chemical inhibitors and dye stuff [11]. Thus the excessive residual of p-AP in environment should be strictly controlled. Therefore, monitoring and selective determination of p-aminophenol becomes more significant to both environmental and human safety aspects. Numbers of methods are used for the determination of p-AP such as HPLC, spectrophotometry, micellar electro kinetic chromatography, capillary electrophoresis and optical fibre reflectance sensor. In this present work, electrochemical method is employed because of their low-cost, simplicity, rapid detection, high sensitivity and selectivity [12].

5.2. EXPERIMENTAL PROCEDURE

5.2.1 Reagents

Silver nitrate ($AgNo_3$), sodium hydroxide (NaOH), sodium borohydride ($NaBH_4$), p-aminophenol are of analytical grade, purchased from sigma Aldrich and are used as received without\ further purification

5.2.2 Synthesis of reduced graphene oxide/ chitosan/Silver nanocomposites

The rGO/CS/Ag nanocomposites are synthesized by dispersing the as prepared rGO/CS solution (as discussed in chapter 2) in 50ml of distilled water by ultrasonication for 1hour to form the aqueous rGO/CS solution [13-14]. The various concentrations of silver nitrate solution (0.002 M, 0.004 M, 0.006 M, 0.008 M and 0.01 M) are stirred separately for 1hour. The stirred silver nitrate solution is then

added dropwise into the above dispersed rGO/CS solution under constant stirring. After 1hour of stirring $NaBH_4$ solution (25 mg) is added dropwise into the above mixture. This reaction mixture is stirred vigorously for 4 hours at 60° C. Thus the formed solution is left undisturbed and the resultant supertant is filtered and washed with distilled water. It is then dried in oven for 4hours at 60° C [15-16].

5.3. RESULTS AND DISCUSSION

5.3.1 FT-IR Spectral Analysis

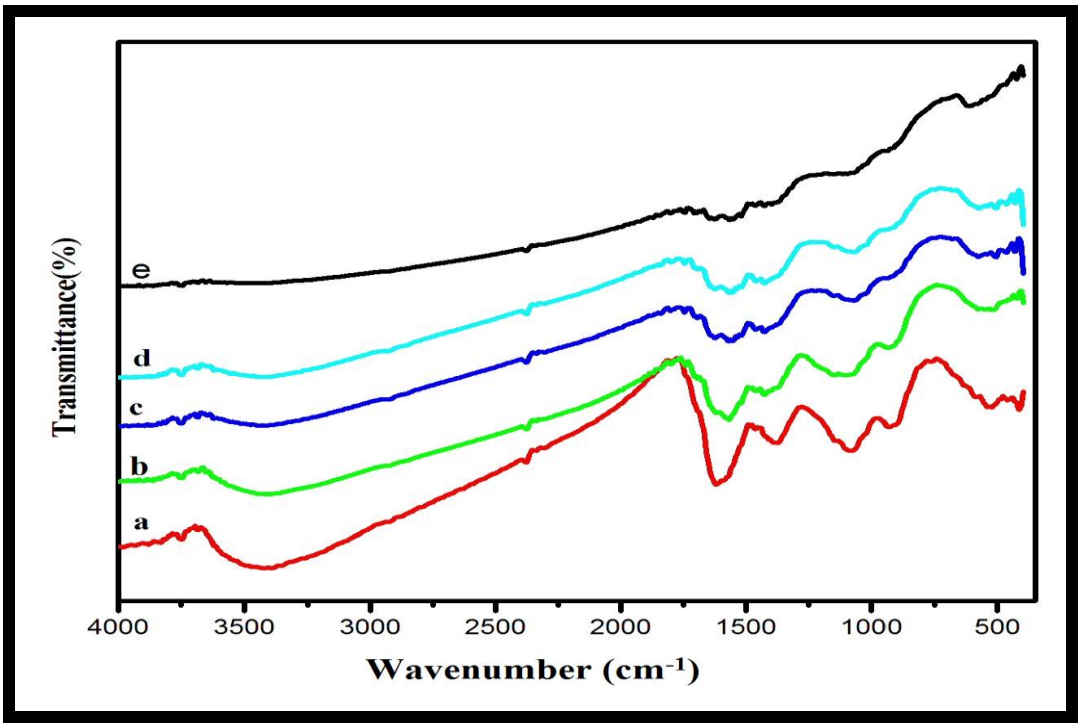

Figure 5.1 (a-e) FT-IR spectral analysis for various concentrations (a) 0.002 M (b) 0.004 M (c) 0.006 M (d) 0.008 M and (e) 0.01 M of silver nanoparticles on the surface of rGO/CS nanocomposites

FT-IR is used to investigate the bonding interactions between the prepared nanocomposites. Figure 5.1 (a-e) shows the FT-IR spectral analysis for various concentrations of silver nitrate 0.002 M, 0.004 M, 0.006 M, 0.008 M and 0.01 M on the surface of rGO/CS nanocomposites. It is observed from Figure 5.1 (a-e) that the band at 3436 cm^{-1} corresponds to the stretching vibration of O-H group. The sharp intense band at1648 cm^{-1} of chitosan attributes to the carbonyl stretching of amide groups. The weak band at 1382 cm^{-1} denoted the symmetric deformation vibrational

mode of C-OH group. The band at 1056 cm^{-1} is due to the alkoxy C-O stretching vibrations. The band formed around 590 cm^{-1} confirms the presence of metallic vibrations in the prepared rGO/CS/Ag nanocomposites [17-18]. On comparing the band of rGO/CS with rGO/CS/Ag the intensity of band at 1648 cm^{-1} decreases with an increase in the intensity of the band at 1056 cm^{-1} which clearly indicates the interaction of amide group of chitosan with silver ions. It is further observed that on increasing the concentration of silver nitrate from 0.002 M to 0.01 M, the intensity of band gets shifted to lower wavenumber indicating the strong interaction between rGO/CS and Ag. It is also observed that on further increasing the concentration of silver nanoparticles the broadness of the bands also increases. These results clearly indicate that silver nanoparticles have been well interacted on the surface of rGO/CS nanocomposites.

5.3.2 XRD Structural Analysis

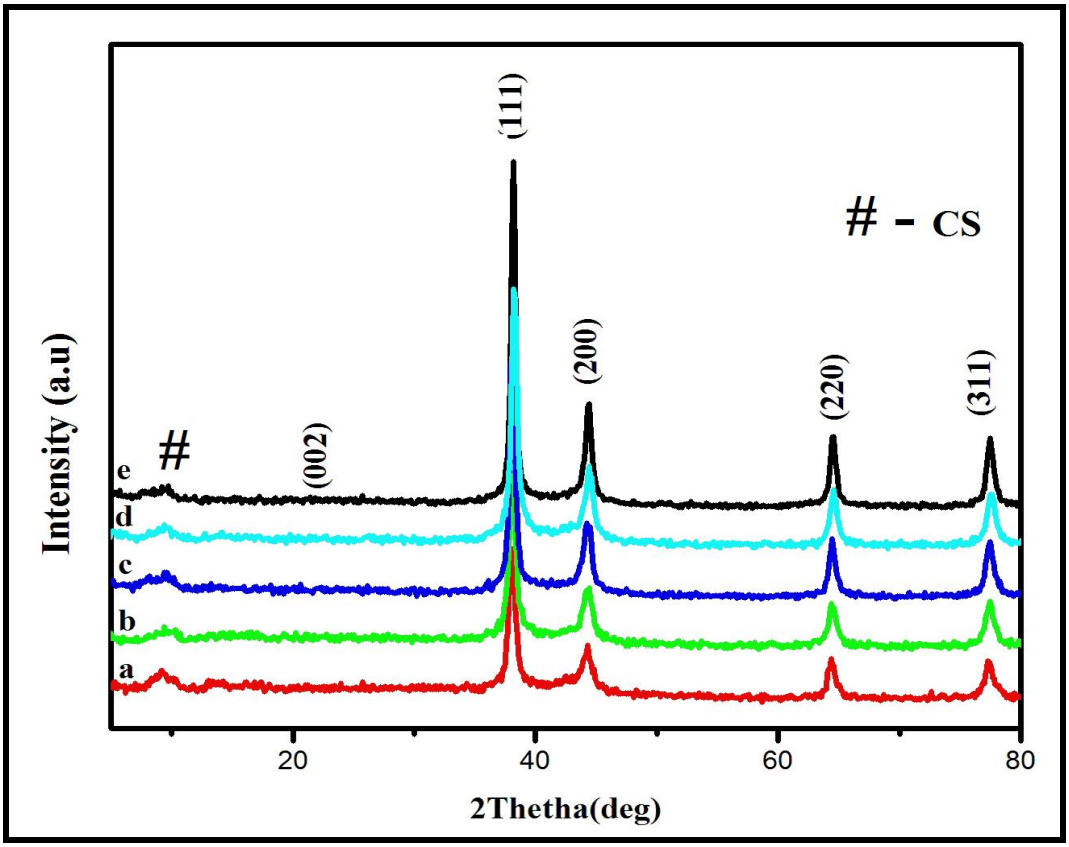

Figure 5.2 (a-e) XRD pattern for various concentrations (a) 0.002 M (b) 0.004 M (c) 0.006 M (d) 0.008 M and (e) 0.01 M of silver nanoparticles on the surface of rGO/CS nanocomposites

The crystalline nature of the prepared rGO/CS/Ag nanocomposites at different concentrations is studied using XRD. Figure 5.2 (a-e) shows the XRD pattern for various concentrations of silver nitrate 0.002 M, 0.004 M, 0.006 M, 0.008 M and 0.01 M on the surface of RGO/CS nanocomposites. The diffraction peaks at 38.2°, 44.2°, 64.6° and 77.1° corresponds to the (111) (200) (220) and (311) planes and are well matched with the JCPDS card number 04-0783 [7]. On increasing the concentration of Ag, the intensity of the peak also increases. The sharpness of the peak suggests that the crystalline nature of Ag nanoparticles. The broad band at 23.6° corresponds to the (002) plane of reduced graphene oxide and the broadening of the peak is due to the amorphous nature of polymer. It is further observed that on increasing the concentration of silver nitrate from 0.002M to 0.01M the intensity of diffraction peaks of silver nanoparticles increases [19-20].

The crystallite size is calculated by using Debye Scherrer's formula and the calculated crystallite size is found to be 17.5 nm, 21.4 nm, 23.5 nm, 23.8 nm and 25.6 nm respectively. It is also observed that the crystallite size increases on increasing the concentration of silver nitrate from 0.002M to 0.01M. These results suggest that the silver nanoparticles are well incorporated onto the surface of rGO/CS nanocomposites.

5.3.3 SEM analysis

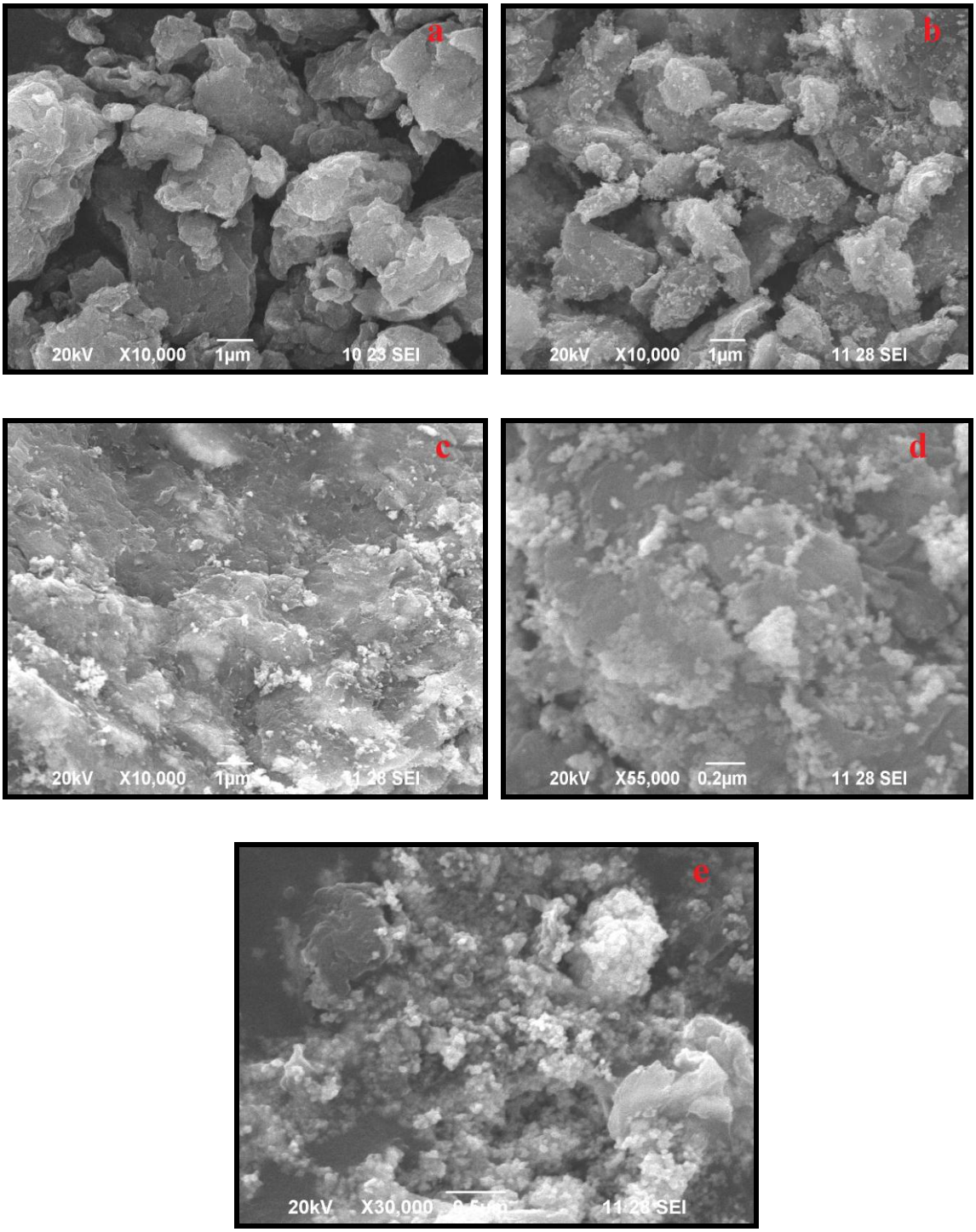

Figure 5.3 (a-e) SEM images of various concentration (a) 0.002 M (b) 0.004 M (c) 0.006 M (d) 0.008 M (e) 0.01 M of silver nanoparticles incorporated on rGO/CS nanocomposites

The surface morphology of the prepared nanocomposites is investigated using scanning electron microscope analysis. Figure 5.3 (a-e) shows the SEM images of various concentration 0.002 M, 0.004 M, 0.006 M, 0.008 M and 0.01 M of silver nanoparticles incorporated on rGO/CS nanocomposites. It is observed from Figure 5.3 (a-e) shows that the spherical shaped silver nanoparticles are well dispersed onto the surface of chitosan modified reduced graphene oxide nanosheets which are closely in contact with each other [21-22]. Moreover on increasing the concentration of silver nitrate from 0.002 M to 0.006 M the number of particles on the surface of rGO/CS nanosheets also increases. On further increase in the concentration of silver nitrate from 0.008 M to 0.01 M the particles on the surface of rGO/CS are found to be agglomerated. This might be due to the heavy loading of silver nanoparticles. These results reveal that silver nanoparticles are well incorporated into the rGO/CS nanosheets.

5.3.4. Energy-Dispersive X-ray analysis

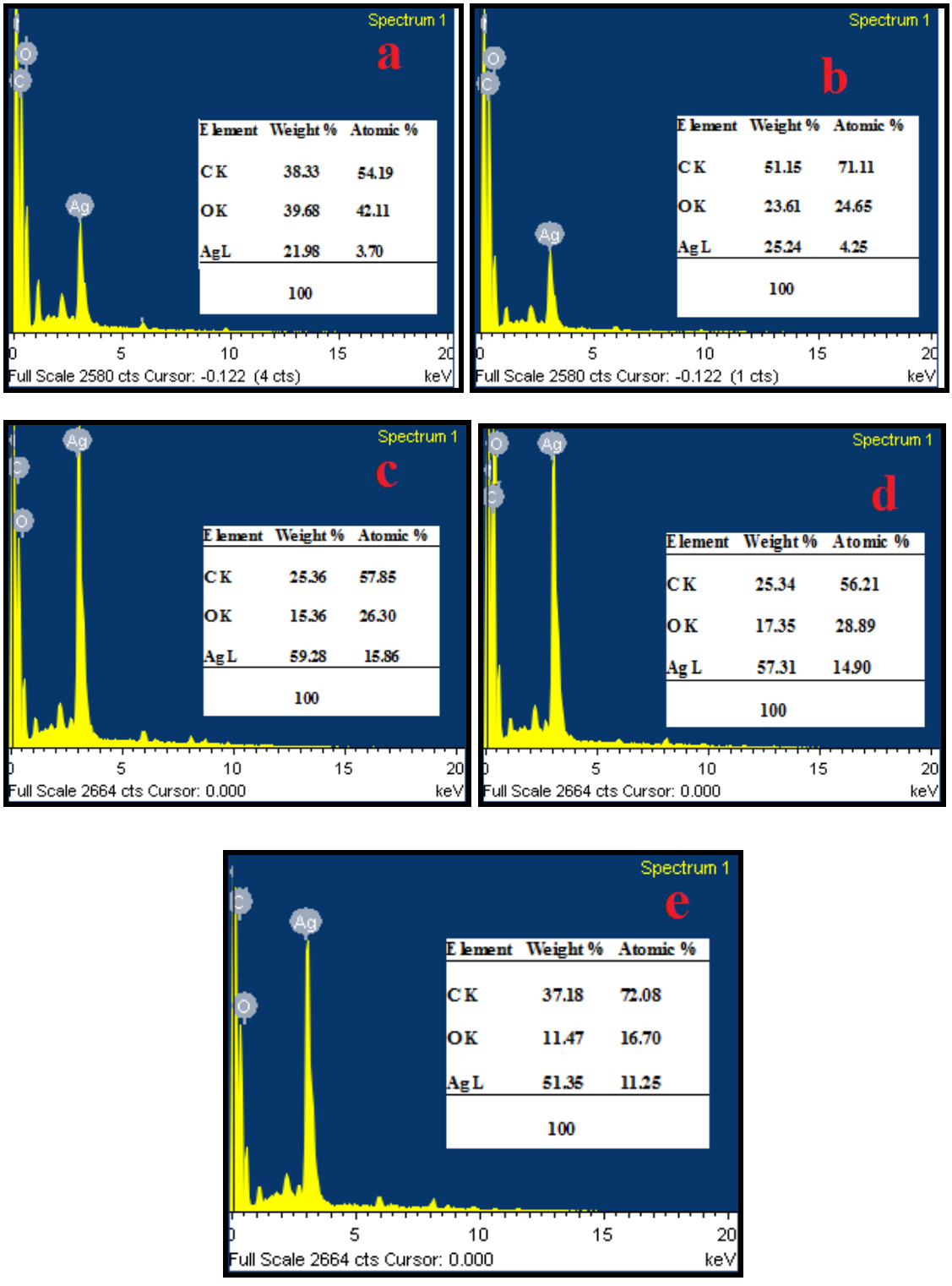

Figure 5.4 (a-e) EDAX spectra for various concentration of (a) 0.002 M (b) 0.004 M (c) 0.006 M (d) 0.008 M (e) 0.01 M of silver nanoparticles incorporated on rGO/CS nanocomposites

The elemental composition of the prepared rGO/CS/Ag nanocomposites is investigated using energy-dispersive X-ray (EDAX) analysis in the range between 0-20KeV binding energy. Figure 5.4 (a-e) shows the EDAX spectra for various concentration of 0.002 M, 0.004 M, 0.006 M, 0.008 M and 0.01 M of silver nanoparticles incorporated on rGO/CS nanocomposites. The presence of carbon, oxygen and silver [23] as depicted from Figure 5.4 (a-e) confirms the formation of RGO/CS/Ag nanocomposites. The quantitative atomic and weight percentage (%) of carbon, oxygen and silver is shown in the inest of Figure 5.4 (a-e). EDAX on mapping with SEM indicates that the weight percentage of Ag nanoparticles loaded on to the surface of RGO/CS is found to be about 21.98, 25.24, 59.28, 57.31 and 51.38. It is observed that the weight percentage of Ag nanoparticles increases with increase in concentration of silver nitrate from 0.002M to 0.006M. On further increase in concentration of silver nitrate, the weight percentage of Ag nanoparticles found to be decreases for 0.008M and 0.01M as evidenced from SEM analysis.

5.3.5 TEM and SAED analysis

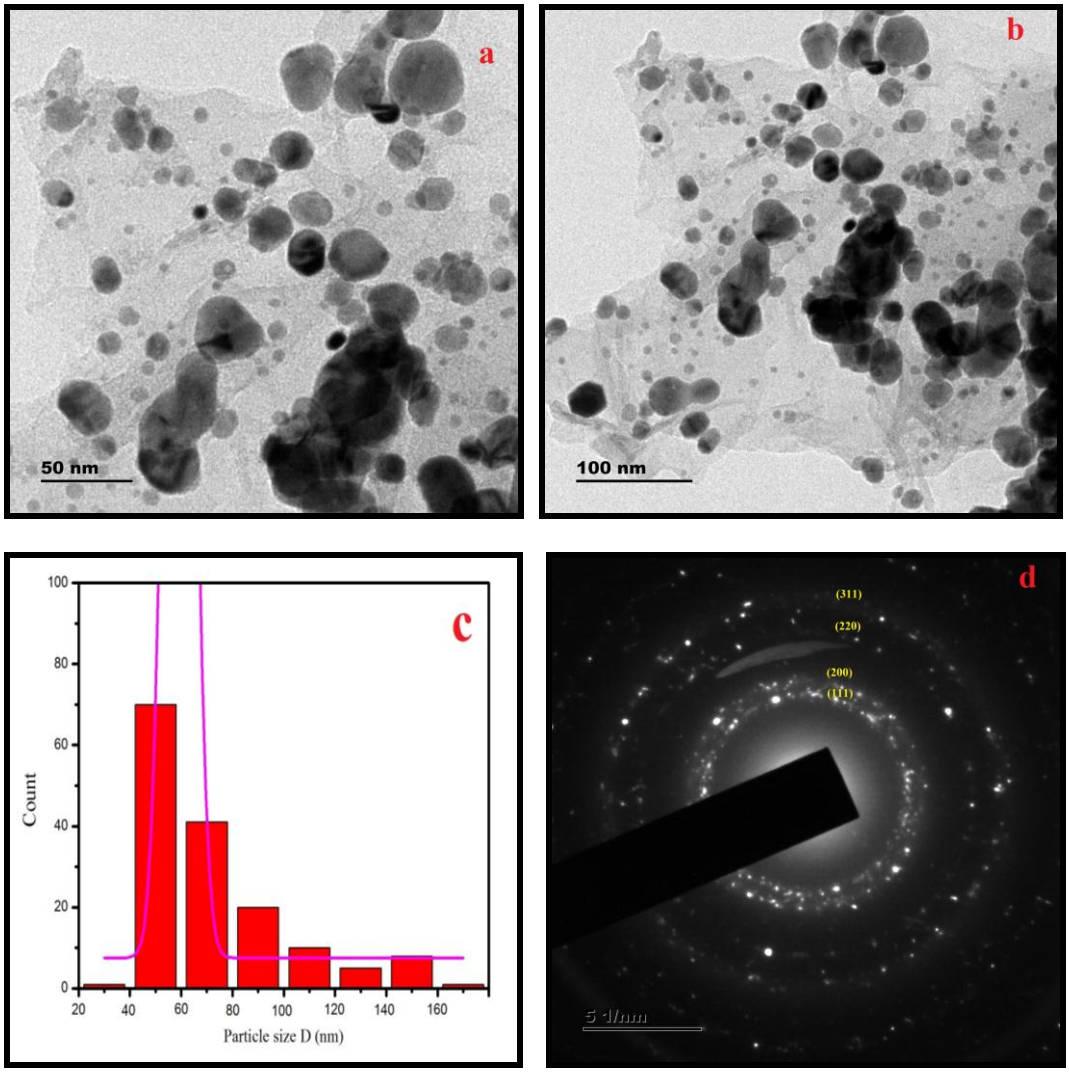

Figure 5.5 (a-b) TEM images for different magnifications and (c) Particle size distribution histogram of rGO/CS/Ag nanocomposites (d) SAED pattern for 0.006M of silver nanoparticles incorporated on rGO/CS nanocomposites

Figure 5.5 (a-b) shows the TEM images for different magnifications of 0.006M of silver nanoparticles incorporated on the rGO/CS nanocomposites. It is observed from Figure 5.5 (a-b) that the spherical shaped silver nanoparticles are well dispersed and closely anchored onto the surface of reduced graphene oxide/chitosan nanosheets. Figure 5.5 (c) shows the particle size distribution histogram of prepared nanocomposites. The size distribution of the Ag nanoparticles is varied in the range of 15-80 nm with the mean diameter of 27.3 nm The SAED pattern of the

rGO/CS/Ag nanocomposites is depicted in Figure 5.5 (d). The SAED pattern shows distinct circular rings indexed as (111), (200), (220) and (311) planes, that is well matched with the JCPDS card no. 04- 0783. These planes correspond to Ag nanoparticles and the dark spots reveal the crystalline nature of the synthesized silver nanoparticles as also evidenced from XRD analysis [24].

5.4. ELECTROCHEMICAL RESPONSE OF p-AMINOPHENOL

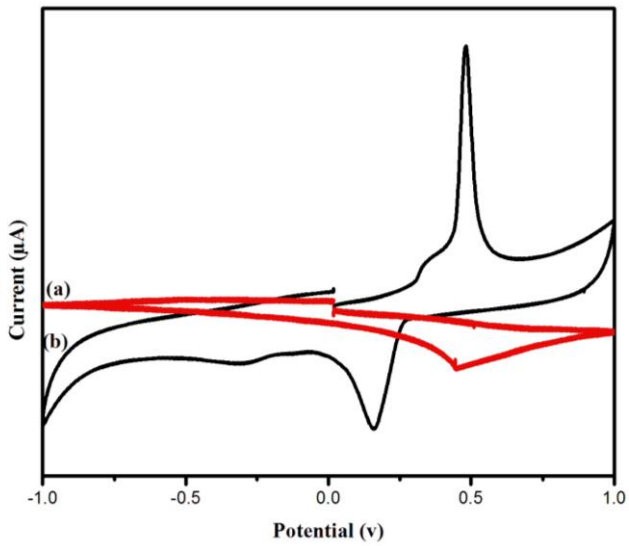

Figure 5.6 (a-b) CV curve for (a) Bare GO and (b) 0.006 M of rGO/CS/Ag modified GCE in absence of p-Aminophenol.

The electrochemical measurements are carried out in the electrolyte solution of 0.1 M phosphate buffer solution (PBS). The electro-chemical behaviour for the prepared GO and rGO/CS/Ag nanocomposites is measured using cyclic voltammetry (CV) and is carried out in PBS solution, at a potential range from -1 to 1 V with a scanning rate of 20 mV/s. Figure 5.6 (a-b) shows the CV curve for bare GO and rGO/CS/Ag modified GCE in absence of p-Aminophenol respectively. No redox peak is observed for GO modified GCE electrode. In contrast a pair of well defined redox peaks is observed at E_{pa} =0.4 V and E_{pc} = 0.15 V for rGO/CS/Ag modified GCE as depicted in the Figure 5.6 (a-b). The peak at 0.48 V can be ascribed to the oxidation of Ag whereas the reduction peak of Ag exhibited at 0.15 V [25]. The strong peak suggests that Ag nanoparticles on the surface of rGO/CS nanosheets improve the conductivity of prepared nanocomposites compared to that of the bare

GO. The proposed rGO/CS/Ag nanocomposites sensor is used for the sensing of p-Aminophenol.

5.4.1 ELECTROCHEMICAL BEHAVIOUR OF MODIFIED ELECTRODES

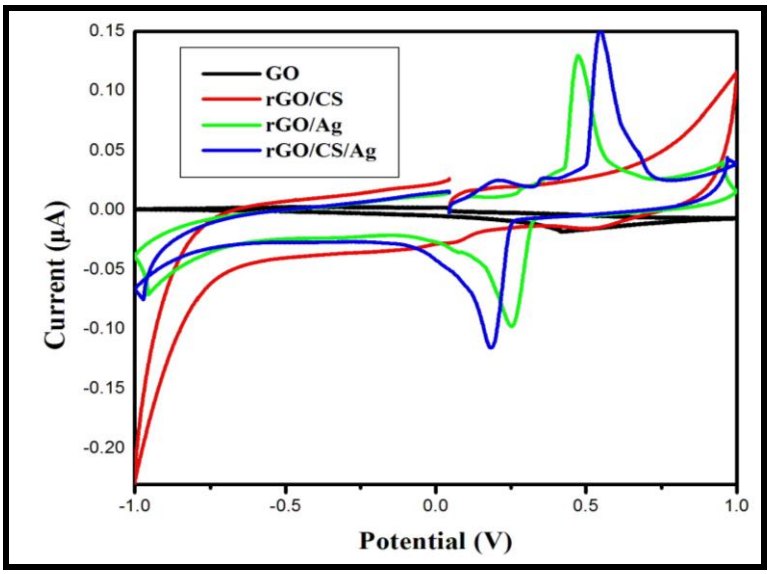

Figure 5.7 (a-d) Cyclic voltagramm curve for (a) GO/GCE (b) rGO/CS/GCE (c) rGO/Ag/GCE and (d) rGO/CS/Ag/GCE in presence of 50µM of p-Aminophenol in 0.1 M Phosphate buffer solution (PBS : pH 6) at a scan rate of 20 mV s^{-1}

The electrochemical behaviour of prepared rGO/CS/Au nanocomposites towards the detection of p-Aminophenol is investigated using cyclic voltammetry. Figure 5.7 (a-d) shows the cyclic voltagramm curve for GO/GCE, rGO/CS/GCE, rGO/Ag/GCE and rGO/CS/Ag/GCE in presence of 50µM of p-Aminophenol in 0.1 M Phosphate buffer solution (PBS: pH 6) at a scan rate of 20 mV s^{-1}. By the addition of 50 µM of p-Aminophenol into the 0.1 M of phosphate buffer solution, no obvious redox peaks is observed for GO modified GCE (GO/GCE) which indicates that GO is not activated towards the sensing of p-Aminophenol. A small sluggish redox peak current of p-Aminophenol at a potential of about E_{pa} = 0.42V and E_{pc} = -0.19V is observed for rGO/CS modified GCE and a pair of weak redox peaks are observed at a potential range of Epa = 0.15 V and Epc = 0.006 V for rGO/Ag modified GCE [9-10]. But for rGO/CS/Ag modified GCE, a pair of well defined redox peaks is observed at a potential of about Epa = 0.009 V. It is further observed

that the current of rGO/CS/Ag nanocomposites is larger than that of both rGO/CS and rGO/Ag nanocomposites indicating the high electron transfer rate of prepared nanocomposites on the electrode.

5.4.2 Effect of pH

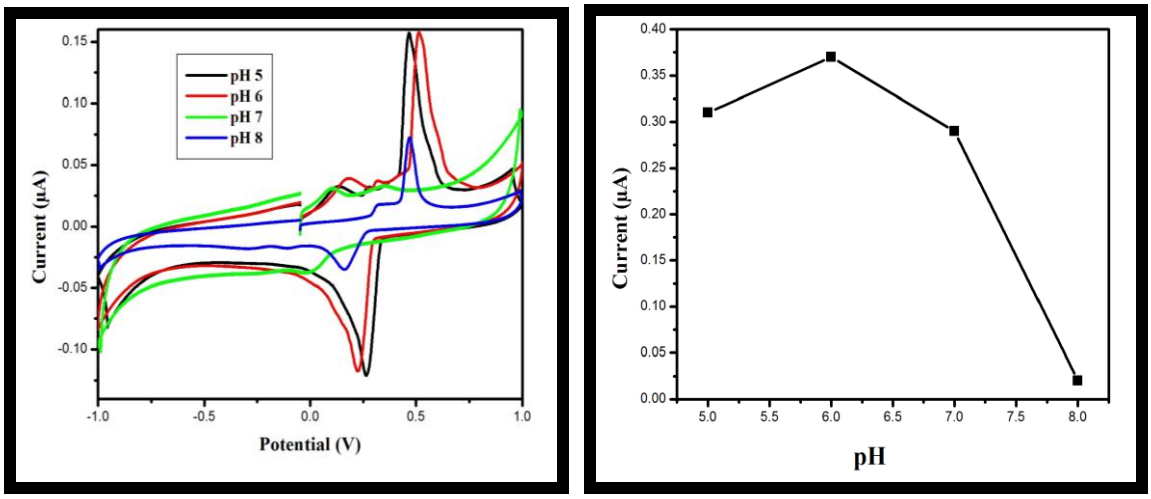

(a) **(b)**

Figure 5.8 (a-b) Effect of pH value of PBS on the redox peak current of 50 µM of p-Aminophenol and its linearity

The effect of pH range (pH 5-8) on the response of 50 µM of p-Aminophenol at rGO/CS/Ag modified GCE is investigated by cyclic voltammetry. Figure 5.8 (a-b) shows the effect of pH value of PBS on the redox peak current of 50 µM of p-Aminophenol and its linearity. It is observed from the figure 5.8 (a) that on increasing the pH from 5 to 8 the oxidation peak current of p-Aminophenol shifts positively and the reduction peak shifts negatively [11]. The relationship of pH to the oxidation peak current (Ipa) of p-Aminophenol is plotted and displayed in Figure 5.8(b). It shows that on increasing the pH from 5 to 6 the oxidation peak current also increases. While on further increase in the pH from 7 to 8, the oxidation peak current decreases and thus pH 6 is chosen as optimum pH for electrochemical sensing of p-Aminophenol.

5.4.3 Effect of scan rate

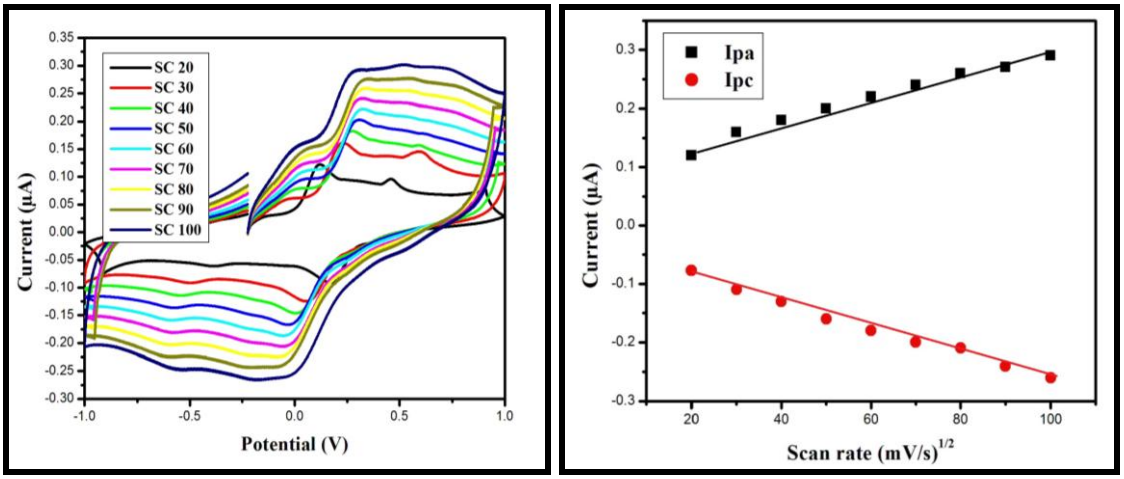

(a) **(b)**

Figure 5.9 (a-b) Cyclic voltagramm curves for effect of scan rate and its linear relationship for 160 µM of p-AP in 0.1 M of PBS solution (pH-6) at various scan rates.

The electrochemical mechanism can be generally acquired from the relationship between the peak current and scan rate subsequently. Figure 5.9 (a-b) shows the cyclic voltagramm curve for effect of scanrate and its linear relationship for 160 µM of p-aminophenol in 0.1 M of PBS solution. It is observed from the Figure 5.9 (a-b) that both the redox peak current of p-Aminophenol increases with increasing the scanrate from 20mV/s to 100mV/s. It clearly indicates that the anionic and cationic peak current increases linearly with scan rate. The graph of I_{pa} and I_{pc} versus scan rate is plotted and shown in Figure 5.9 (b). The resultant graph shows excellent linearity for electrochemical sensing of p-Aminophenol. It is further observed that the anodic current shifts positively and the cathodic current shifts negatively which shows that the electrode process is diffusion controlled process [11].

5.4.4 Effect of analyte concentration

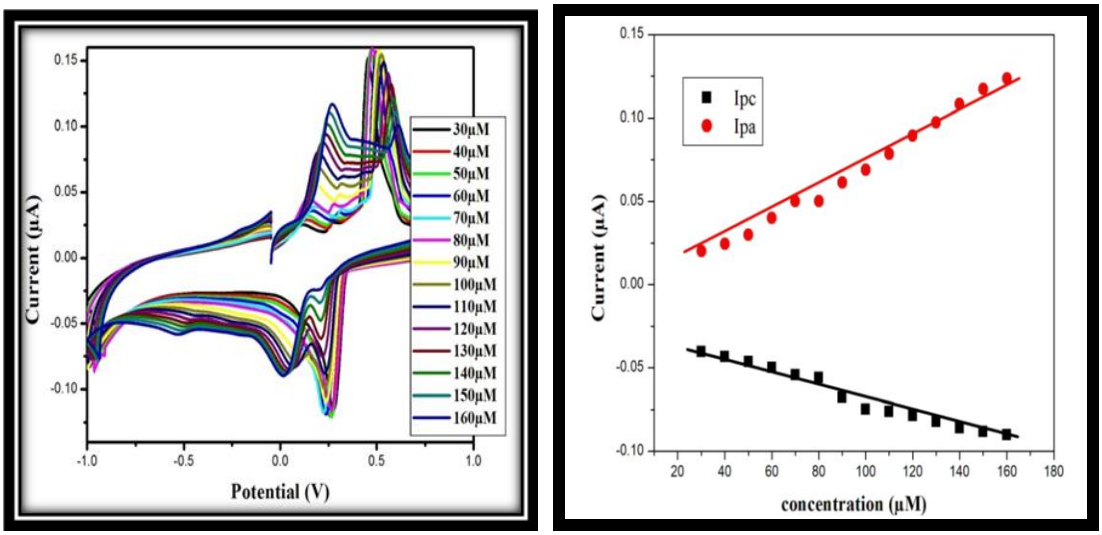

(a) **(b)**

Figure 5.10 (a-b) Cyclic voltagramm curves for 0.006M of rGO/CS/Ag/GCE towards the detection of p-Aminophenol in 0.1 M of PBS solution (pH 6) at a scan rate of 20 mV/s and its linearity

The electrochemical measurements towards the detection of p-Aminophenol on rGO/CS/Ag nanocomposites modified GCE is performed using cyclic voltammetry (CV) under the same experimental conditions. CV is recorded at a potential range of -1 V to 1 V. Figure 5.10 (a-b) shows the cyclic voltagramm curves for 0.006M of rGO/CS/Ag/GCE towards the detection of various concentration of p-Aminophenol and its linearity. It is observed that on increasing the concentration of p-Aminophenol from 30 µM to 160 µM, the redox peak current of p-Aminophenol also increases linearly with a wide linear range of about 30 µM to 160 µM. This increase in the current indicates a good electro catalytic activity of the prepared nanocomposites. Thus the enhanced electro catalytic activity is due to the synergistic contribution of the efficient conductivity of rGO/CS and high loading of Ag nanoparticles onto the rGO/CS sheets [26]. These results indicate that the prepared nanocomposites showed a good response over the detection of p-Aminophenol.

5.5 CONCLUSION

The rGO/CS/Ag nanocomposites are synthesized by chemical reduction method and are well characterized by XRD, FT-IR, SEM and EDAX analysis. The stretching vibration of N-H band at 1640 cm^{-1}confirms the interaction of GO with CS. The metallic band formed around 596 cm^{-1} confirms the formation of Ag nanoparticles on the surface of rGO/CS. The crystallite size of the formed nanocomposites is about 23.6 nm. The crystallite size increases on increasing the Ag concentration. The surface morphological studies reveal that the spherical shaped Ag nanopartices are well dispersed on the thin crumbled leaf like rGO/CS sheets. EDAX analysis confirms the presence of elements without any impurities and the formation of rGO/CS/Ag nanocomposites. SAED pattern confirms the crystalline nature of the prepared nanocomposites. The rGO/CS/Ag modified GCE electrode exhibits a high current for pH 6 of about 0.11μA and wide linear range of 30 μM to 160μM for p-Aminophenol. The results reveal that the large effective surface area of the prepared nanocomposites allows it to function as an electron transfer medium and enhances the charge transfer rate. Thus the rGO/CS/Ag modified GCE shows good electrocatalytic activity towards the detection of p-Aminophenol. Thus the proposed electrochemical sensor can be potentially applied in environment for the detection of p-Aminophenol.

REFERENCES

1. Yue Lin, Jie Jin and Mo Song, Preparation and characterisation of covalent polymer functionalized graphene oxide, J. Mater. Chem., 21, 3455–3461 | 3455, (2011)

2. Abdullahi Mohamed Farah, Force Tefo Thema and Ezekiel Dixon Dikio, Electrochemical Detection of Hydrogen Peroxide Based on Graphene Oxide/Prussian Blue Modified Glassy Carbon Electrode, Int. J. Electrochem. Sci., 7 5069 – 5083, (2012)

3. Sijie Wan, Feiyu Xu, Lei Jiang and Qunfeng Cheng, Adv. Funct. Mater1605636, (2017)

4. Fatemeh Emadi, AbbasAmini, Ahmad Gholami and YounesGhasemi, Functionalized Graphene Oxide with Chitosan for Protein Nanocarriers to Protect against Enzymatic Cleavage and Retain Collagenase Activity, Scientific Reports, 7:42258, (2017).

5. Hongqian Bao , Yongzheng Pan , Yuan Ping , Nanda Gopal Sahoo , Tongfei Wu , Lin Li, Jun Li and Leong Huat Gan , Chitosan-Functionalized Graphene Oxide as a Nanocarrier for Drug and Gene Delivery*7*, No. 11, 1569–1578, (2011)

6. S. Govindan, E. A. K. Nivethaa, R. Saravanan, V. Narayanan and A. Stephen, Synthesis and characterization of chitosan–silver nanocomposite, Appl Nanosci 2:299–303,(2012).

7. Indranil Roy, Dipak Rana, Gunjan Sarkar, Amarty, Bhattacharyya, Nayan Ranjan Saha, Soumya Mondal, Sutanuka Pattanayak, Sanatan Chattopadhyay, Dipankar and Chattopadhyay, Physical and electrochemical characterization of reduced graphene oxide/silver nanocomposites synthesized by adopting green approach, RSC Adv., 00, 1-8, (2015).

8. Wenjing Lian, SuLiu, JinghuaYu, JieLi, MinCui, WeiXu and JiadongHuang, Electrochemical sensor using neomycin-imprinted film as recognition element based on chitosan-silvernanoparticles/graphene-multiwalled carbonnanotubes composites modified electrode, Biosensors and Bioelectronics 44,70–76, (2013).

9. Junjuan Qian, Depeng Zhang, Lirong Liu, Yinhui Yi, Mwenze Nkulu Fiston, Odoom Jibrael Kingsford and Gangbing Zhu, Carbon Spheres Wrapped with Molybdenum Disulfide Nanostructure for Sensitive Electrochemical Sensing of 4-aminophenol, Journal of The Electrochemical Society, 165B491-B497, (2017).

10. Yasemin Oztekin, Almira Ramanaviciene and Arunas Ramanavicius, Electrochemical Glutathione Sensor Based on Electrochemically deposited Poly-m-aminophenol, Electroanalysis 23, No. 3, 701 – 709, (2011).

11. J.Vinoth Kumar, R.Karthik, Shen-Ming Chen, K.Saravanakumar1, Govindasamy Mani, V.Muthuraj, Novel hydrothermal synthesis of MoS_2 nanoclusters structure for sensitive electrochemical detection of human and environmental hazardous pollutant 4-aminophenol, RSC Adv., DOI:10.1039/C6RA03343A, (2016).

12. Dong Sun, Xiaokun Li, Huajie Zhang and Xiafeng Xie , An electrochemical sensor for p-aminophenol based on the mesoporous silica modified carbon paste electrode, Intern. J. Environ. Anal. Chem.Vol. 92, No. 3, 15, 324–333, (2012).

13. Ulises Antonio Méndez Romero,Miguel Ángel Velasco Soto, Liliana Licea Jiménez, Jaime Álvarez Quintana and Sergio Alfonso Pérez García, Graphene Derivatives: Controlled Properties, Nanocomposites, and Energy Harvesting Applications, http://dx.doi.org/10.5772/67474, 77-96.

14. Jianguo Song, Xinzhi Wang and Chang-Tang Chang, Preparation and Characterization of Graphene Oxide, Journal of Nanomaterials, http://dx.doi.org/10.1155/2014/276143, (2014).

15. Paulchamy , Arthi and Lignesh, A Simple Approach to Stepwise Synthesis of Graphene Oxide Nanomaterial, Journal of Nanomed and Nanotechnology, DOI: 10.4172/2157-7439.1000253, (2015).

16. Mingming Wan, Zhiming Liu, Shaoxin Li, Biwen Yang, Wen Zhang, Xiaochu Qin, Zhouyi Guo, Silver nanoaggregates on Chitosan Functionalized Graphene Oxide for High-Performance Surface-Enhanced Raman Scattering, Society for Applied Spectroscopy, 10.1366/12-06777, (2013).

17. Leila shahriary and anjali a. Athawale, Graphene oxide synthesized by using modified hummers approach, International Journal of Renewable Energy and Environmental Engineering, ISSN 2348-0157, Vol. 02, No. 01, (2014).

18. Yazhou Zhou , Juan Yang , Tingting He, Haifeng Shi , Xiaonong Cheng and Yuxin Lu, Highly Stable and Dispersive Silver Nanoparticle–Graphene Composites by a Simple and Low-Energy Consuming Approach and Their Antimicrobial Activity, small, DOI: 10.1002/smll.201202455, (2013).

19. D. Depan, T. C. Pesacret and R. D. K. Misra, The synergistic effect of a hybrid graphene oxide–chitosan system and biomimetic mineralization on osteoblast functions, Biomater. Sci., 2, 264, (2014).

20. Renu Pasricha, Shweta Gupta and Avanish Kumar Srivastava, A Facile and Novel Synthesis of Ag–Graphene-Based Nanocomposites, Small micro nano communications, https://doi.org/10.1002/smll.200900726, (2009).

21. N.I. Zaaba, K.L. Foo, U. Hashim, .J.Tan, Wei-Wen Liu, C.H. Voona, Synthesis of Graphene Oxide using Modified Hummers Method Solvent Influence, Science Direct, Procedia Engineering 184, 469 – 477, (2017).

22. Santhana Krishna Kumara and Shiuh-Jen Jianga, Chitosan-functionalized graphene oxide: A novel adsorbent an efficient adsorption of arsenic from aqueous solution, http://dx.doi.org/doi:10.1016/j.jece.2016.02.035, (2016).

23. Nithya Arjunan, Henry Linda Jeeva Kumari, Chandra Mohan Singaravelua, Ruckmani Kandasamy and Jothivenkatachalam Kandasamya, Physicochemical investigations of biogenic chitosan-silver nanocomposite as antimicrobial and anticancer agent, International Journal of Biological Macromolecules 92, 77–87(2016).

24. Truong Thi Tuong Vi, Selvaraj Rajesh Kumar, Bishakh Rout, Chi-Hsien Liu ID , Chak-Bor Wong , Chia-Wei Chang , Chien-Hao Chen, Dave W. Chen and Shingjiang Jessie Lue , The Preparation of Graphene Oxide-Silver Nanocomposites: The Effect of Silver Loads on Gram-Positive and Gram-Negative Antibacterial Activities, Nanomaterials, 8, 163, (1-15) (2018).

25. Trupti R. Das, Rashmi Madhuri, and Prashant K. Sharma, Electrocatalytic activity of silver nanoparticles decorated reduced graphene oxide (AgNP@rGO) nanocomposites, : AIP Conference Proceedings, http://dx.doi.org/10.1063/1.4980248, (2017).

26. PolymerYong Liu, Kai Yan, BinWang, Changzhu Yang and Jingdong Zhang, An Electrochemical Sensor for Selective Detection of *p*-Aminophenol Using Hemin-Graphene Composites and Molecularly Imprinted, Journal of The Electrochemical Society, 164 (14) B776-B780, (2017).